

Optically Governed Dynamic Surface Charge Redistribution of Hybrid Plasmo-Pyroelectric Nanosystems

Chi Hao Liow, Xin Lu, Kaiyang Zeng, Shuzhou Li, and Ghim Wei Ho*

Though plasmonic effect is making some headway in the energy harvesting realm, its fundamental charge transfer mechanism to a large extent is attributed to the hot-carrier generation at the contact interface. Herein this work attempts to elucidate the physical origin of light induced plasmo-pyroelectric enhancement based on charge density manipulation on surface state in the vicinity of the metal-ferroelectric contact interface. More importantly, by tuning the band bending, it is shown that the charge density on the surface state of a hybrid plasmo-pyroelectric (BaTiO₃-Ag) nanosystem can be manipulated and largely increased under the resonant blue light illumination (363 nm). It is also demonstrated that owing to this effect, the spatial pyroelectric activity of a hybrid plasmo-pyroelectric nanosystem governs 46% enhancement in pyroelectric coefficient. This research highlights the optically regulated charge density in plasmo-pyroelectric nanosystems, which could pave a new avenue for energy harvesting/conversion devices with distinguished advantages in wireless, photonic-controlled, localized, and dynamic stimulation.

Light-activated pyroelectric energy conversion has garnered immense interest in a wide span of applications, including nanogenerators,^[1–4] heat and infrared sensors,^[5] and thermal imaging.^[6] When light illuminates pyroelectric materials, such as LiNbO₃, Pb(Zr,Ti)O₃, BiFeO₃, and BaTiO₃ (BTO),^[7–10] the noncentrosymmetric materials undergo oscillation in their

electric dipoles that decreases the amount of bound charge. This leads to redistribution of free charge to compensate the variation of the bound charge and generates a current flow.^[11] As the performance of an energy harvester is related to its charge density, significant efforts have been made to increase the charge density by means of poling, material selection, architecture optimization, and surface modification.^[12,13]

More recently, with band bending alteration, the flow direction of optically excited electrons was demonstrated to be controllable in ferroelectric-metal systems,^[10,11,14–16] which has further expanded the potential strategies to manipulate the charge density of the materials. However, due to the wide bandgap (2.7–4 eV) of ferroelectric materials, they absorb less than 20% of the solar spectrum, resulting in unfavorable low charge density.^[17]

In view of the strong light absorption characteristics of plasmonic nanomaterials, hybrid plasmo-pyroelectric nanosystem is a particularly interesting route to exploit the pivotal effect of charge variation on the pyroelectric performance. When a metallic nanoparticle comes into electrical contact with a metal-oxide material, the charge will redistribute to reach a new equilibrium by re-aligning their Fermi energies, which can be observed from the contact potential difference.^[18–20] With a selective wavelength-dependence characteristic, the net charge state of a plasmonic nanoparticle on metal-oxide can be either positive or negative.^[21,22] Although much work has been done on optically excited charge transfer in metal-ferroelectric systems,^[11,14,23,24] the relationship between plasmonic-induced surface charge and pyroelectric activity remains elusive.

In this paper, we highlight the surface charge variation under different light illumination based on a BTO-Ag nanosystem. By integrating light source equipped with different wavelength filters into Kelvin probe force microscopy (KPFM), the influence of light illumination on BTO and BTO-Ag was observed in situ. We found that the local surface potential of a positively poled BTO-Ag induced by blue light illumination far exceeds that of nonpoled, negatively poled, and green light illuminated BTO-Ag nanosystems. Through a combination of electrodynamic simulation and electronic band structure, the working mechanism of surface charge manipulation is unveiled. Under positive poling, the partial-ohmic contact of hybrid BTO-Ag nanosystem switches to a Schottky contact, which enhances charge separation. In addition, the plasmonic field augments


Dr. C. H. Liow, X. Lu, Prof. G. W. Ho
Department of Electrical and Computer Engineering
National University of Singapore
4 Engineering Drive 3, Singapore 117583, Singapore
E-mail: elehwg@nus.edu.sg

Prof. K. Zeng
Department of Mechanical Engineering
National University of Singapore
9 Engineering Drive 1, Singapore 117576, Singapore

Prof. S. Li
School of Materials Science and Engineering
Nanyang Technological University
50 Nanyang Avenue, Singapore 639798, Singapore

Prof. G. W. Ho
Engineering Science Programme
National University of Singapore
9 Engineering Drive 1, Singapore 117575, Singapore

Prof. G. W. Ho
Institute of Materials Research and Engineering
A*STAR (Agency for Science, Technology and Research)
3 Research Link, Singapore 117602, Singapore

 The ORCID identification number(s) for the author(s) of this article can be found under <https://doi.org/10.1002/sml.201903042>.

DOI: 10.1002/sml.201903042

the electron–hole pairs generation to fill the surface state in the immediate vicinity of the BTO–Ag interface, resulting in electron drift and an increase in surface potential. This process is determined to be a dominant factor that governs about 46% pyroelectric response enhancement in the hybrid BTO–Ag nanosystem under resonant visible illumination. Our observation of plasmo-pyroelectric enhancement effect is anticipated to impact the prospective plasmonic integrated ferroelectric driven technologies.

The hydrothermally prepared BTO nanocubes are shown in **Figure 1**. From the scanning electron microscope (SEM) image (Figure 1a), the average size of BTO nanocubes is estimated to be around 90 nm, as confirmed by the transmission electron microscope (TEM) images shown in Figure S1 (Supporting Information). The hybrid BTO–Ag nanosystem was materialized via photodeposition of Ag nanoparticles onto the surface of BTO at various BTO:Ag⁺ molar ratio (0–2.5), as described in our previous work (Figure 1b, Figure S2, Supporting Information).^[25] As the molar ratio of BTO:Ag⁺ increases, the size of deposited Ag nanoparticles also increases correspondingly.

The noncentrosymmetric structure of BTO can be observed from X-ray diffraction (XRD) diffractogram (Figure 1c), where

the tetragonal phase with *P4mm* space group can be determined from the split peak at 45°. ^[26,27] Clearly, photodeposition of Ag does not alter the BTO lattice structure in the hybrid nanosystem. The electronic structure and optical properties of BTO were further analyzed using density functional theory (DFT) with spin polarization and Hubbard *U* correction (Figure S3, Supporting Information). The calculated bandgap between conduction band and valence band is ≈2.7 eV (Figure S3b, Supporting Information), which is very close to the value derived from Tauc plot (≈2.9–3.3 eV) (Figure S4, Supporting Information). From the projected density of states (PDOS), it is obvious that the conduction and valence bands near the Fermi level are predominated by Ti 3d and O 2p, which indicates the crucial role of hybridization of Ti 3d and O 2p in BTO tetragonal phase formation, as previously reported.^[28] Due to the slight displacement of Ti atom in the center of BTO unit cell, the complex dielectric function exhibits a uniaxial characteristic, which is shown in Figure S3a (Supporting Information).

Figure 2a illustrates the optical absorption of BTO and hybrid BTO–Ag nanosystems. By incorporating the DFT calculated dielectric function (Figure S5, Supporting Information) into electrodynamic calculation, we obtained a good

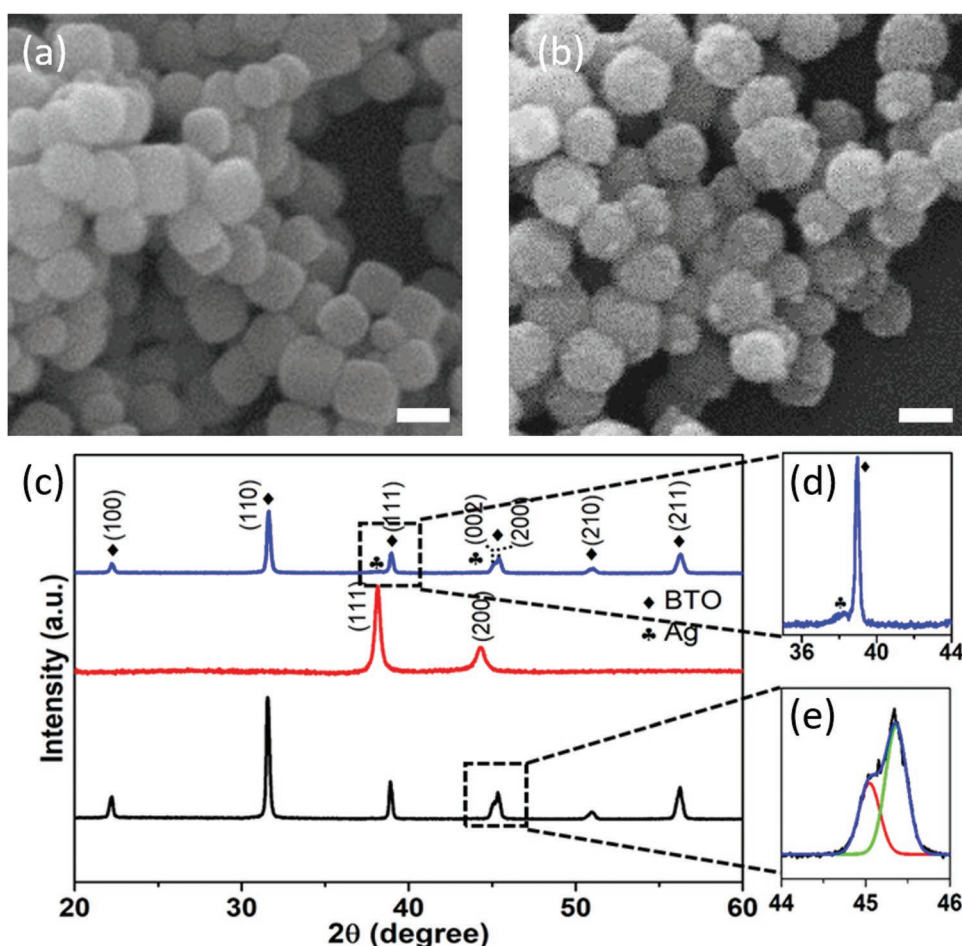


Figure 1. a) SEM image of BTO nanocubes synthesized using hydrothermal method. b) SEM image of BTO–Ag at molar ratio of 1:2.5. Scale bar of SEM image is 100 nm. c) XRD diffraction of BTO, Ag, and hybrid BTO–Ag. d) Enlarged portion of BTO–Ag nanosystem, the small peak indicates the presence of Ag in the hybrid system; however, due to the low concentration of Ag relative to BTO, Ag peaks in the hybrid nanosystem appear to be much weaker than that of BTO peaks. e) A peak split around 45° indicates tetragonal phase of as-synthesized BTO nanoparticles.

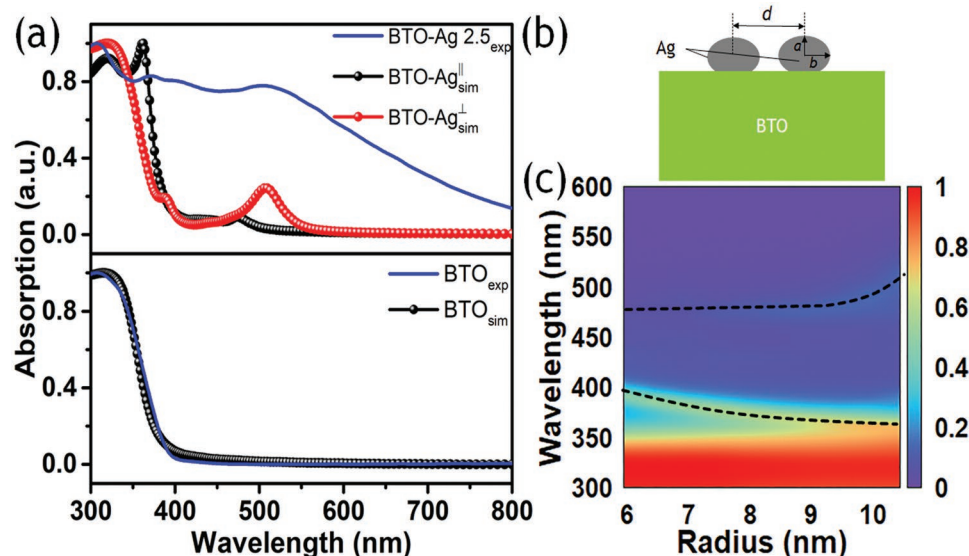


Figure 2. Optical properties comparison of BTO and BTO-Ag obtained by UV-vis measurement and FDTD calculation a) (top) BTO-Ag 2.5_{exp} is the experimental measured absorption and BTO-Ag_{sim}^{||} (BTO-Ag_{sim}[⊥]) is the FDTD calculated absorption at parallel (perpendicular) incident light with respect to the BTO-Ag interface. (bottom) BTO_{exp} is the experimentally measured absorption and BTO_{sim} is the FDTD calculated absorption. b) Schematic illustration of FDTD model used for electrodynamic simulation. c) Plasmonic resonance map calculated by FDTD at both light incident directions against the increase of radius, b . The dotted lines represent guides to the eye.

agreement between the calculated and the experimental results. Henceforth, the DFT calculated dielectric function of BTO will be used for all the subsequent hybrid BTO-Ag electrodynamic simulations. The hybrid structure is modeled as an Ag solid spheroid on a BTO cube. According to Gans theory, the plasmonic resonance wavelength is strongly dependent on geometry aspect ratio (a/b) and its adjacent dielectric environment. In this study, we investigate the coupling effect between two Ag nanoparticles by increasing the particle radius, with a fixed distance of 24 nm between their centers, as shown in Figure 2b. The map of plasmonic resonance shifts illustrated in Figure 2c agrees qualitatively with the observed experimental absorption (Figure 3a) for different Ag⁺ molar ratio. In general, as the density of Ag nanoparticles increases, we observed a blue shift to the higher energy plasmonic resonance with a concurrent red shift to the lower energy plasmonic resonance. Considering that the plasmonic resonance is geometry dependent, the anisotropic nanoparticles will generate both longitudinal and transverse plasmonic oscillation along a -axis and b -axis respectively. As the aspect ratio increases at b -axis, the retardation effect is stronger at the longer wavelength, hence inducing a red shift. Simultaneously, this geometry change also results in a blue shift in plasmonic resonance at the shorter wavelength.

In order to elucidate the influence of light on the poled hybrid BTO-Ag nanosystem, KPFM equipped with light source was employed to probe in situ changes in the charge density based on surface potential at a nanometer-level spatial resolution. Here, the contact potential difference (V_{cpd}) between the tip and the sample surface is calculated by: $(W_{\text{tip}} - W_{\text{sample}})/e$, where W_{tip} and W_{sample} represent the respective work function of the tip and sample respectively, and e is the elementary charge (1.6×10^{-19} C).^[29] To prevent the tip-induced band bending effect, the KPFM tip was operated at a hover height of 30 nm above the sample. W_{tip} was calibrated with a freshly

cleaved pyrolytic graphite (HOPG) substrate with a work function of 4.475 eV as a reference. In the KPFM configuration, positive changes in V_{cpd} represents a net increase in the negative charge (electron density) on the sample surface, and vice versa. Since plasmonic excitation can be controlled by the frequency of the incident light, the plasmonic resonance-enhanced pyroelectric effect on the energy conversion can be systematically studied. Figure 3b and Figure S6 (Supporting Information) show the respective topography and phase images of BTO-Ag at molar ratio 2.5 measured by atomic force microscopy (AFM). Figure 3c–e shows the V_{cpd} mapping under different illuminations (blue (363 nm), green (530 nm)) and dark condition, respectively. In contrast to green illumination and dark condition, a pronounced positive V_{cpd} is observed under blue illumination, which indicates an increase in electron density of the hybrid nanosystems. The effect of light illumination on the poled (positively and negatively poled) nanosystems can be determined by subtracting the average V_{cpd} under dark condition from that of the illuminated one ($\Delta V_{\text{cpd}} = V_{\text{cpd}}(\text{light}) - V_{\text{cpd}}(\text{dark})$), as shown in Figure 3f. It is interesting to note that only blue light illumination on positively poled hybrid nanosystem results in a significant increase in surface potential, while green light illumination results in a slight decrease in surface potential across different Ag⁺ molar ratio. Conversely, for the case of negatively poled nanosystem, both light illumination result in an increase in their surface potential by different magnitudes. These results evidently present a direct optically modulated surface potential of ferroelectric–metal nanosystem by varying the charge density of poled hybrid nanosystem utilizing incident light of different wavelengths.

Here, we calculate the optical generation rates (G) with parallel (530 nm) and perpendicular (363 nm) light polarizations as illustrated in Figure 4. G represents the number of photogenerated carriers at each point per unit time. For both

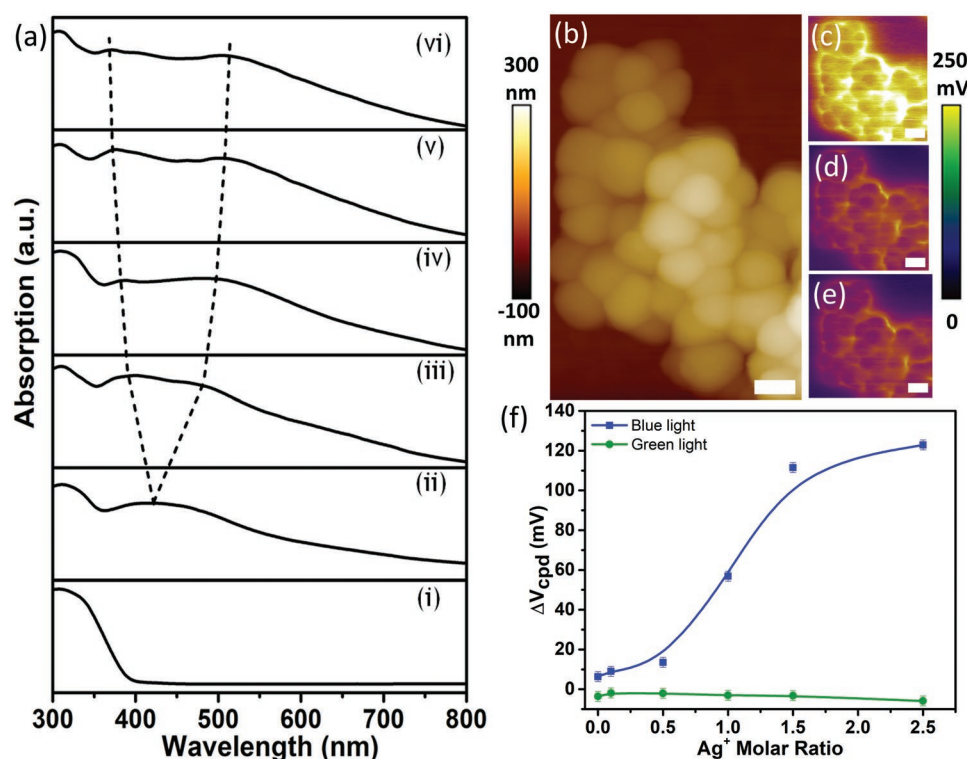


Figure 3. a) UV-vis spectra of BTO and BTO-Ag at different molar ratio i) BTO ii) BTO: Ag 1: 0.1 iii) BTO: Ag 1: 0.5 iv) BTO: Ag 1: 1.0 v) BTO: Ag 1: 1.5 vi) BTO: Ag 1: 2.5. b) AFM topographic images of BTO-Ag at molar ratio of 2.5 c,d) V_{cpd} maps of BTO-Ag under blue (363 nm) and green (530 nm) light illuminations, while e) is measured in dark. Scale bar is 100 nm. f) V_{cpd} difference of poled BTO and BTO-Ag nanosystem calculated in relative to their respective dark condition. The solid lines represent the best fit.

polarizations, a large G is observed at the interface of the BTO-Ag and the intensity decreases gradually with increasing distance from BTO-Ag interface. This proves that the influence of plasmonic resonance is not only limited to the interface, but also extends to the surrounding of the BTO core. From the result, we also observed that as the wavelength of incident light moves closer to the plasmonic resonance of BTO-Ag, a larger G can be obtained and vice versa (Figure 4c,d and Figure 2a). From the above discussion, it is clear that the photogeneration surface charge enhancement is sensitive to the incident light because of plasmonic resonance; however, it still does not explicitly explain the physical insight of light to the stimulated magnitude of ΔV_{cpd} at their respective poling conditions.

There are two possible explanations for the light induced surface potential manipulation in the hybrid nanosystem, namely, light-induced plasmoelectric effect^[21,22] and light-induced polarization switching in ferroelectric material.^[19] First, poling results in a screening charge accumulation on the surface of ferroelectric material, which could serve as a charge reservoir for plasmoelectric effect. If plasmoelectric effect takes place, charge density reduction is expected under illumination of lower energy light, in relation to their plasmonic resonance. However, this phenomenon is not observed especially in negatively poled ones. Second, we carried out piezoresponse force microscopy in illuminated and dark conditions in order to investigate the influence of light on polarization switching in BTO-Ag (Figure 4e). Clearly, the directions of polarization remained unchanged in both conditions, allowing us to rule

out the possibility of light-induced polarization switching. Therefore, we put forth the postulation that band bending alteration in the hybrid nanosystem has facilitated an easier pathway for the electrons to occupy the vicinity surface states, resulting in significant change in the surface potential. In the nonpoled BTO-Ag nanosystem, electrons will diffuse from the lower workfunction Ag (-4.3 eV) to BTO (-5.3 eV) to form an equilibrium state (Figure 5a,b).^[30] With blue light illumination, electron transfer between metal and BTO due to excitation of hot electrons and excitons occur simultaneously. However, from the increase in ΔV_{cpd} (Figure 4f), we can conclude that electron transfer from BTO to the surface state is the dominant process. Contrarily, the ΔV_{cpd} decreases under green light illumination. Since only Ag plasmonic resonance is excited, the decrease can be attributed to the electrons discharging from Ag to BTO. For a negatively poled BTO-Ag nanosystem, negative screening charges will build up to yield a downward band bending (Figure 5c,d), while positive poling results in positive screening bound charges which cause a significant upward band bending between Ag and BTO (Figure 5e,f).^[15] The band bending observed in negative poling is similar to that without poling, but of a greater magnitude. Under blue light illumination, an electron transfer pathway similar to the nonpoled counterparts is established. Interestingly, the green light illumination also resulted in the increase of ΔV_{cpd} , which signifies the back-transfer of electrons from BTO to Ag.^[29] As the back-transfer of electrons is not observed in nonpoled nanosystem, we postulate that negative poling has facilitated a steeper

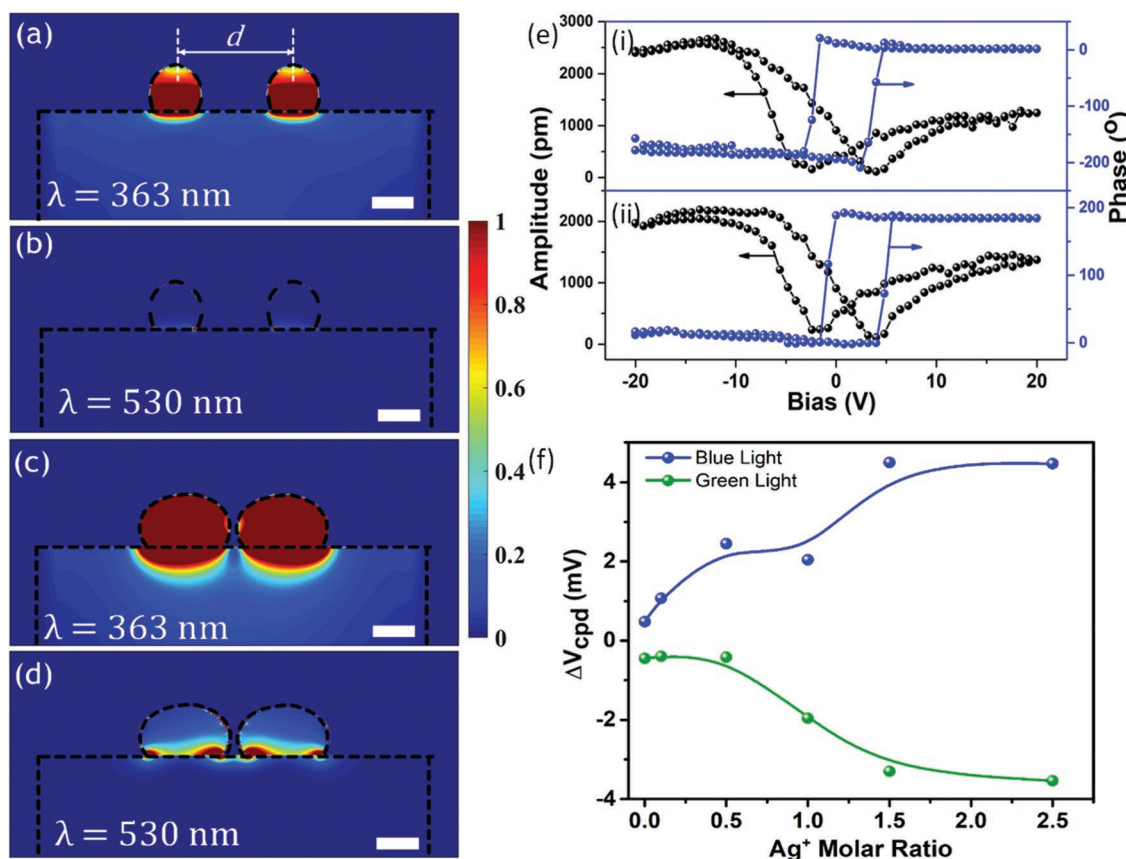


Figure 4. The calculated cross sectional distribution of the optical generation rate (G) at their respective incident wavelength with a,c) perpendicular b,d) parallel polarization directions. The centers between two Ag nanoparticles are positioned at distance of 24 nm (d) and the radius of Ag are 6 and 10.5 nm for a,b) and c,d), respectively. The scale bar is 10 nm. The color bar is an intensity indication of normalized G . e) Piezoresponse force microscopy measurement of BTO-Ag at 2.5 molar ratio under i) dark and ii) full spectrum light illumination. f) ΔV_{cpd} of nonpoled BTO and BTO-Ag nanosystems calculated in relative to their respective dark condition. The solid lines represent the best fit.

energy band that favors the electron back transfer. In the case of positive poling, upward band bending is induced, accompanied by a large depletion width (ΔW) (Figure S7, Supporting Information). At a molar ratio of 2.5, ΔW is calculated to be as large as ≈ 60 nm from the interface. By exciting the plasmonic resonance, enhanced electric field enables more electron-hole pairs to be generated as discussed earlier, leading to effective diffusion of electrons to the surface state of the BTO-Ag before recombination.^[31] Upon blue light illumination, not only has the photogenerated electrons increased, but the plasmonic resonance of Ag nanoparticle is also triggered, allowing the vicinity electrons to drift near to the metallic nanoparticles, thus inducing significant changes in the surface potential.^[20] While with green light illumination, the loss of electrons is attributed to the hot-electron injection into the BTO (Figure 4f), as observed in the nonpoled nanosystem.

Next, we evaluate the dynamics of surface charge manipulation based on a positively poled plasmopyroelectric nanosystem under the influence of light illumination. Figure 6 shows the local pyroelectric response of the hybrid nanosystem in the absence and presence of full spectrum light, summarized from Figure S8 (Supporting Information). As expected, the measured pyroelectric coefficient follows the observed ΔV_{cpd} trends in Figure 3f. Intuitively, the results suggested that the

resonant blue light illumination plays a dominant factor in determining the performance of hybrid BTO-Ag nanosystem. For more clarity on this phenomenon, we categorize the pyroelectric response into R1, R2, and R3. In R1, due to the small ΔW and hot-electron injection, the surface state is largely unoccupied by electrons, which lowers the charging magnitude, hence leading to a low pyroelectric response. As the Ag^+ molar ratio increases, we enter region R2 where the photogeneration of electron-hole pairs in BTO starts to dominate and gradually occupies the empty surface state. Since the charging capability is linearly correlated to the size of the metallic nanoparticle,^[29,32] the pyroelectric response in R2 also increased linearly. Lastly, in R3, as the ΔW is reaching its plateau (Figure S7, Supporting Information), the charge separation also exhibits a similar pattern. Even with the presence of larger Ag nanoparticle, the magnitude of the charging will be limited by occupied surface states, hence resulting in the plateau characteristics of the pyroelectric response. Therefore, instead of hot-electron injection that only occurs at the interface between Ag and BTO, the occupancy of electrons on the surface state is a predominant factor that governs the pyroelectric coefficient under full spectrum light illumination, which leads to 46% enhancement at molar ratio of 2.5.

In conclusion, we observed a direct manipulation of ΔV_{cpd} in the hybrid BTO-Ag nanosystem probed at nanoscale utilizing

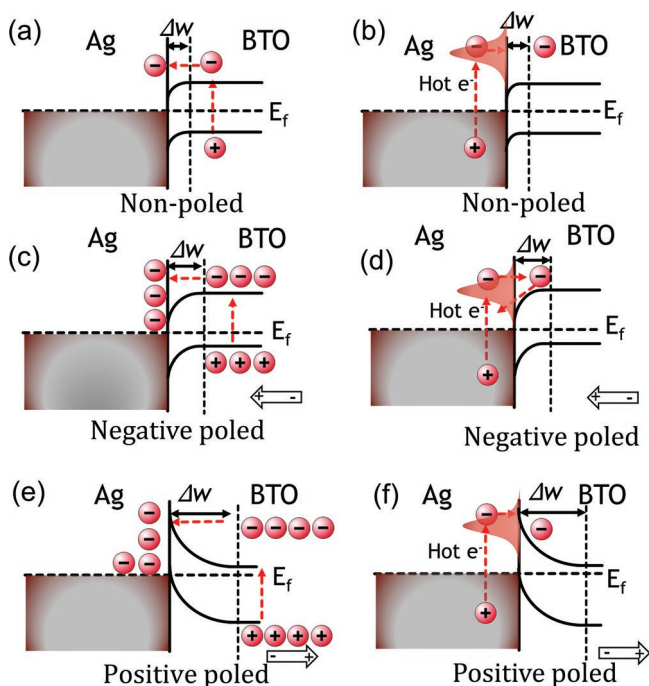


Figure 5. Schematic illustration of light induced (blue (363 nm)-left column and green (530 nm)-right column) electron transfer pathways in BTO–Ag nanosystems with different poled conditions a) and b) are nonpoled; c) and d) are negatively poled; e) and f) are positively poled.

in situ KPFM with light illumination. We found that the poled hybrid BTO–Ag nanosystem exhibits a large ΔV_{cpd} under resonant blue light illumination. Together with the plasmonic effect and the electronic band bending, the optically induced change in ΔV_{cpd} is unveiled based on electron occupancy on the surface state of the hybrid nanosystem. Lastly, through the dynamic fluctuation of pyroelectric material, we demonstrated

that the participation of charge on the surface state plays a crucial role in enhancing the pyroelectric coefficient of the hybrid plasmo-pyroelectric nanosystem. We anticipate that the insight provided by this study will be useful in the design of plasmon-ferroelectric optoelectronic and energy harvesting technologies.

Supporting Information

Supporting Information is available from the Wiley Online Library or from the author.

Acknowledgements

C.H.L. and X.L. contributed equally to this work. The authors thank Hao Wei for his guidance in density functional theory calculations. This research is supported by the Singapore Ministry of National Development and the National Research Foundation, Prime Minister's Office under the Land and Liveability National Innovation Challenge (L2 NIC) Research Programme (L2 NIC Award No. L2NICCFP2-2015-3).

Conflict of Interest

The authors declare no conflict of interest.

Keywords

energy harvesting enhancement, plasmonic, poling, pyroelectric, surface charge density

Received: June 12, 2019

Revised: July 4, 2019

Published online: July 24, 2019

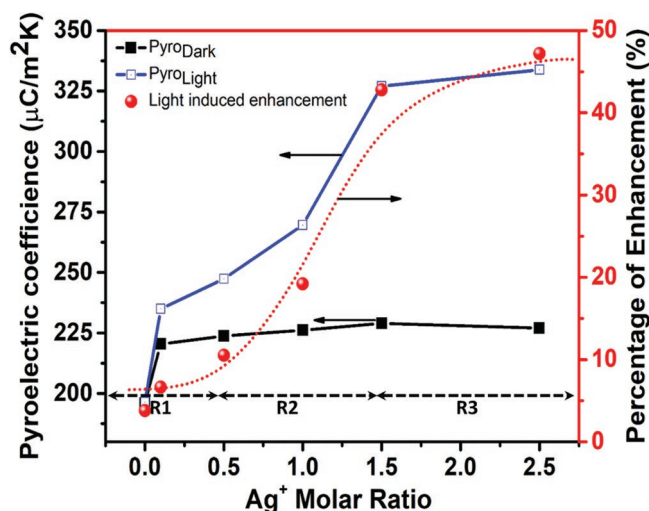


Figure 6. Measured pyroelectric coefficient of BTO and hybrid BTO–Ag nanosystems under full spectrum wavelength illumination at constant temperature fluctuation ($\Delta T = 1$ K). R1 < 0.5 molar Ag^+ deposition, 0.5 molar < R2 < 1.5 molar Ag^+ deposition, and R3 > 1.5 molar Ag^+ deposition.

- [1] C. M. Shiran, D. Tordera, A. Grimaldi, I. Engquist, M. Berggren, S. Fabiano, M. P. Jonsson, *Adv. Opt. Mater.* **2018**, 6, 1701051.
- [2] T. P. Ding, L. L. Zhu, X. Q. Wang, K. H. Chan, X. Lu, Y. Cheng, G. W. Ho, *Adv. Energy Mater.* **2018**, 8, 1802397.
- [3] C. H. Liow, L. Xin, T. C. Fu, C. K. Hoe, Z. Kaiyang, L. Shuzhou, H. G. Wei, *Small* **2018**, 14, 1702268.
- [4] X. Q. Wang, C. F. Tan, K. H. Chan, K. C. Xu, M. H. Hong, S. W. Kim, G. W. Ho, *ACS Nano* **2017**, 11, 10568.
- [5] T. D. Dao, S. Ishii, T. Yokoyama, T. Sawada, R. P. Sugavaneshwar, K. Chen, Y. Wada, T. Nabatame, T. Nagao, *ACS Photonics* **2016**, 3, 1271.
- [6] J. Park, M. Kim, Y. Lee, H. S. Lee, H. Ko, *Sci. Adv.* **2015**, 1, e1500661.
- [7] A. M. Glass, D. V. D. Linde, T. J. Negran, *Appl. Phys. Lett.* **1974**, 25, 233.
- [8] S. Y. Yang, J. Seidel, S. J. Byrnes, P. Shafer, C. H. Yang, M. D. Rossell, P. Yu, Y. H. Chu, J. F. Scott, J. W. Ager III, L. W. Martin, R. Ramesh, *Nat. Nanotechnol.* **2010**, 5, 143.
- [9] J. Zhang, X. Su, M. Shen, Z. Shen, L. Zhang, X. Zhang, W. Cheng, M. Cao, G. Zou, *Sci. Rep.* **2013**, 3, 2109.
- [10] N. Ma, K. Zhang, Y. Yang, *Adv. Mater.* **2017**, 29, 1703694.
- [11] K. Song, N. Ma, Y. K. Mishra, R. Adelung, Y. Yang, *Adv. Electron. Mater.* **2019**, 5, 1800413.
- [12] S. Pandya, J. Wilbur, J. Kim, R. Gao, A. Dasgupta, C. Dames, L. W. Martin, *Nat. Mater.* **2018**, 17, 432.

- [13] Y. Yang, S. H. Wang, Y. Zhang, Z. L. Wang, *Nano Lett.* **2012**, 12, 6408.
- [14] N. Ma, K. W. Zhang, Y. Yang, *Adv. Mater.* **2017**, 29, 1703694.
- [15] Z. J. Wang, D. W. Cao, L. Y. Wen, R. Xu, M. Obergfell, Y. Mi, Z. B. Zhan, N. Nasori, J. Demsar, Y. Lei, *Nat. Commun.* **2016**, 7, 10348.
- [16] M. Shiran Chaharsoughi, D. Zhao, X. Crispin, S. Fabiano, M. P. Jonsson, *Adv. Funct. Mater.* **2019**, 0, 1900572.
- [17] A. Bhatnagar, A. R. Chaudhuri, Y. H. Kim, D. Hesse, M. Alexe, *Nat. Commun.* **2013**, 4, 2835.
- [18] Z. Zhang, J. T. Yates Jr., *Chem. Rev.* **2012**, 112, 5520.
- [19] T. Li, A. Lipatov, H. D. Lu, H. Lee, J. W. Lee, E. Torun, L. Wirtz, C. B. Eom, J. Iniguez, A. Sinitskii, A. Gruverman, *Nat. Commun.* **2018**, 9, 3344.
- [20] D.-B. Li, X.-J. Sun, Y.-P. Jia, M. I. Stockman, H. P. Paudel, H. Song, H. Jiang, Z.-M. Li, *Light: Sci. Appl.* **2017**, 6, e17038.
- [21] J. van de Groep, M. T. Sheldon, H. A. Atwater, A. Polman, *Sci. Rep.* **2016**, 6, 23283.
- [22] M. T. Sheldon, J. van de Groep, A. M. Brown, A. Polman, H. A. Atwater, *Science* **2014**, 346, 828.
- [23] N. Ma, Y. Yang, *Nano Energy* **2017**, 40, 352.
- [24] B. Chen, J. Shi, X. Zheng, Y. Zhou, K. Zhu, S. Priya, J. Mater. Chem. A **2015**, 3, 7699.
- [25] W. L. Ong, S. Natarajan, B. Kloostera, G. W. Ho, *Nanoscale* **2013**, 5, 5568.
- [26] K. I. Park, M. Lee, Y. Liu, S. Moon, G. T. Hwang, G. Zhu, J. E. Kim, S. O. Kim, D. K. Kim, Z. L. Wang, K. J. Lee, *Adv. Mater.* **2012**, 24, 2999.
- [27] N. Nuraje, K. Su, A. Haboosheh, J. Samson, E. P. Manning, N. L. Yang, H. Matsui, *Adv. Mater.* **2006**, 18, 807.
- [28] F. Maldonado, A. Stashans, *J. Phys. Chem. Solids* **2017**, 102, 136.
- [29] S. H. Lee, S. W. Lee, T. Oh, S. H. Petrosko, C. A. Mirkin, J. W. Jang, *Nano Lett.* **2018**, 18, 109.
- [30] S. Zhang, B.-p. Zhang, S. Li, Z. Huang, C. Yang, H. Wang, *J. Adv. Ceram.* **2017**, 6, 1.
- [31] B. Chen, J. Shi, X. J. Zheng, Y. Zhou, K. Zhu, S. Priya, J. Mater. Chem. A **2015**, 3, 7699.
- [32] Y. J. Zhang, O. Pluchery, L. Caillard, A. F. Lamic-Humblot, S. Casale, Y. J. Chaba, M. Salmeron, *Nano Lett.* **2015**, 15, 51.